

# A possible sea-level fall trigger for the youngest rejuvenated volcanism in Hawai'i

## Brian R. Jicha<sup>1,†</sup>, Michael O. Garcia<sup>2</sup>, and Charline Lormand<sup>3</sup>

- <sup>1</sup>Department of Geoscience, University of Wisconsin-Madison, Madison, Wisconsin, 53706, USA
- <sup>2</sup>Department of Earth Sciences, University of Hawai'i, Honolulu, Hawai'i, 96822, USA

#### **ABSTRACT**

Many intraplate oceanic islands undergo "rejuvenated" volcanism following the main edifice-building stage. Honolulu features Hawai'i's most recent rejuvenated volcanism. K-Ar dating of Honolulu volcanism suggests that it started at ca. 750 ka and ended at <100 ka. Here, we present new <sup>40</sup>Ar/<sup>39</sup>Ar ages and olivine diffusion modeling from Koko Rift lavas to resolve when the most recent Honolulu eruptions occurred and to evaluate possible mechanisms of rejuvenated volcanism and volcanic hazards. Diffusion modeling of olivine zoning profiles in Koko Rift basalts suggests that magmas were stored in the crust for many months prior to eruption. Six new 40Ar/39Ar ages cluster at  $67 \pm 2$  ka  $(2\sigma)$ , which demonstrates that Koko Rift is Hawai'i's youngest known area of rejuvenated volcanism. The timing of Koko Rift eruptions coincides with the pronounced drop in global sea level (~100 m) during Marine Isotope Stage 4. This major sea-level fall may have triggered the eruptions of Koko Rift magmas that were stored in the crust for months to years at <15 km depth. The proposed mechanism is similar to that at other volcanic islands, which suggests that changes in global sea level may have significant control on the magnitude and frequency of eruptions at ocean island volcanoes.

## INTRODUCTION

Rejuvenated volcanism is an enigmatic aspect of hotspot magmatism that occurs hundreds of kilometers downstream from the ascending mantle plume stem following an eruptive hiatus. Many oceanic island groups have rejuvenated

Brian Jicha https://orcid.org/0000-0002-1228-

†brian.jicha@wisc.edu.

volcanism, including Samoa (Konter and Jackson, 2012), Kerguelen (Weis et al., 1998), Madeira (Geldmacher and Hoernle, 2000), Mauritius (Paul et al., 2005), and Hawai'i (Garcia et al., 2016). Dana (1849) was the first to recognize the "secondary" nature of Diamond Head and the many other cones in the Honolulu area. Dutton (1884) suggested that these cones formed after a long hiatus in volcanism. The duration, number of eruptions, and extent of rejuvenation volcanism on the Hawaiian Islands is variable, ranging from brief (0.2-0.3 Ma) episodes with only a few cones on the younger Hawaiian Islands (Maui and Moloka'i) to >2 Ma periods with extensive on- and off-shore cones for the older northern islands (Ka'ula, Ni'ihau, and Kaua'i; Garcia et al., 2016).

Rejuvenated volcanism on the Hawaiian Islands is also episodic in nature, with gaps of tens to hundreds of thousands of years between eruptions (Ozawa et al., 2005; Garcia et al., 2010). Honolulu contains Hawai'i's most recent rejuvenated volcanism (Dana, 1849), and it remains unclear whether there could be future volcanism in the Honolulu area. Critically important to answering this question is knowing the age(s) of its most recent volcanism and the longer-term frequency of eruptions. Geologic mapping has shown that two Honolulu areas, Koko Rift on the southeastern corner of the island and Tantalus Rift (~4 km east of downtown Honolulu; Fig. 1), have the most recent volcanism on Oahu based on their deposits overlying carbonates from the Marine Isotope Stage 5e (or MIS 5.5) sea-level high stand (Wentworth, 1926). The compositions of lavas from these two rifts are at the extremes of the compositional range for Honolulu Volcanics (melilite nephelinite for Tantalus and weakly alkalic basalt for Koko Rift; Winchell, 1947; Clague and Frey, 1982). Thus, the two eruptive sequences are unrelated. 40Ar/39Ar methods were used to date K-rich nepheline from a Tantalus Rift flow and yielded a plateau age of  $76 \pm 2$  ka ( $2\sigma$ ; Clague et al., 2016). This age is consistent with previously published K-Ar data (e.g., Ozawa et al., 2005; Gramlich et al., 1971) and with U-Th ages for the carbonate deposits that underlie this flow and the Koko Rift deposits (ca. 114–131 ka; Szabo et al., 1994).

Attempts to date Koko Rift eruptions using K-Ar methods have produced a broad range of ages (34-320 ka; Gramlich et al., 1971; Lanphere and Dalrymple, 1980; Ozawa et al., 2005), most of which have large uncertainties. 40Ar/39Ar ages ( $60 \pm 50$ – $140 \pm 100$  ka) were obtained for three somewhat altered samples from the submarine southwestern end of Koko Rift (Clague et al., 2006). These results have large uncertainties (±50-100 ka), non-atmospheric isochron intercepts, and two of the three samples analyzed have disturbed age spectra with high mean squares of weighted deviates (MSWDs; 2.4-4.0). The discrepancies amongst K-Ar ages generated by multiple laboratories as well as between various geochronologic methods (40Ar/39Ar vs. K-Ar) for Koko Rift lavas attest to the difficulty in dating young mafic lavas (e.g., Heizler et al., 1999; Preece et al., 2018). This is primarily due to the limited quantity of radiogenic <sup>40</sup>Ar\* that is difficult to distinguish from large amounts of trapped atmospheric argon. We obtained 40Ar/39Ar ages and olivine diffusion modeling for subaerial Koko Rift lavas to: (1) determine when the last eruptions in Honolulu occurred, (2) evaluate possible models and triggers of rejuvenated volcanism, and (3) assess the potential for future eruptions.

The petrology of Koko Rift basalts, including textural and mineral chemical data, was recently published by Garcia et al. (2022). This work cited geochronologic data from an "in review manuscript" by B. Jicha that was ultimately not published. All new Koko Rift <sup>40</sup>Ar/<sup>39</sup>Ar data, figures, analytical details, interpretations, and implications are presented herein. Moreover, the detailed compositional profiles and olivine

https://doi.org/10.1130/B36615.1; 5 figures; 1 table; 1 supplemental file.

<sup>&</sup>lt;sup>3</sup>Department of Earth Sciences, Durham University, Durham, UK

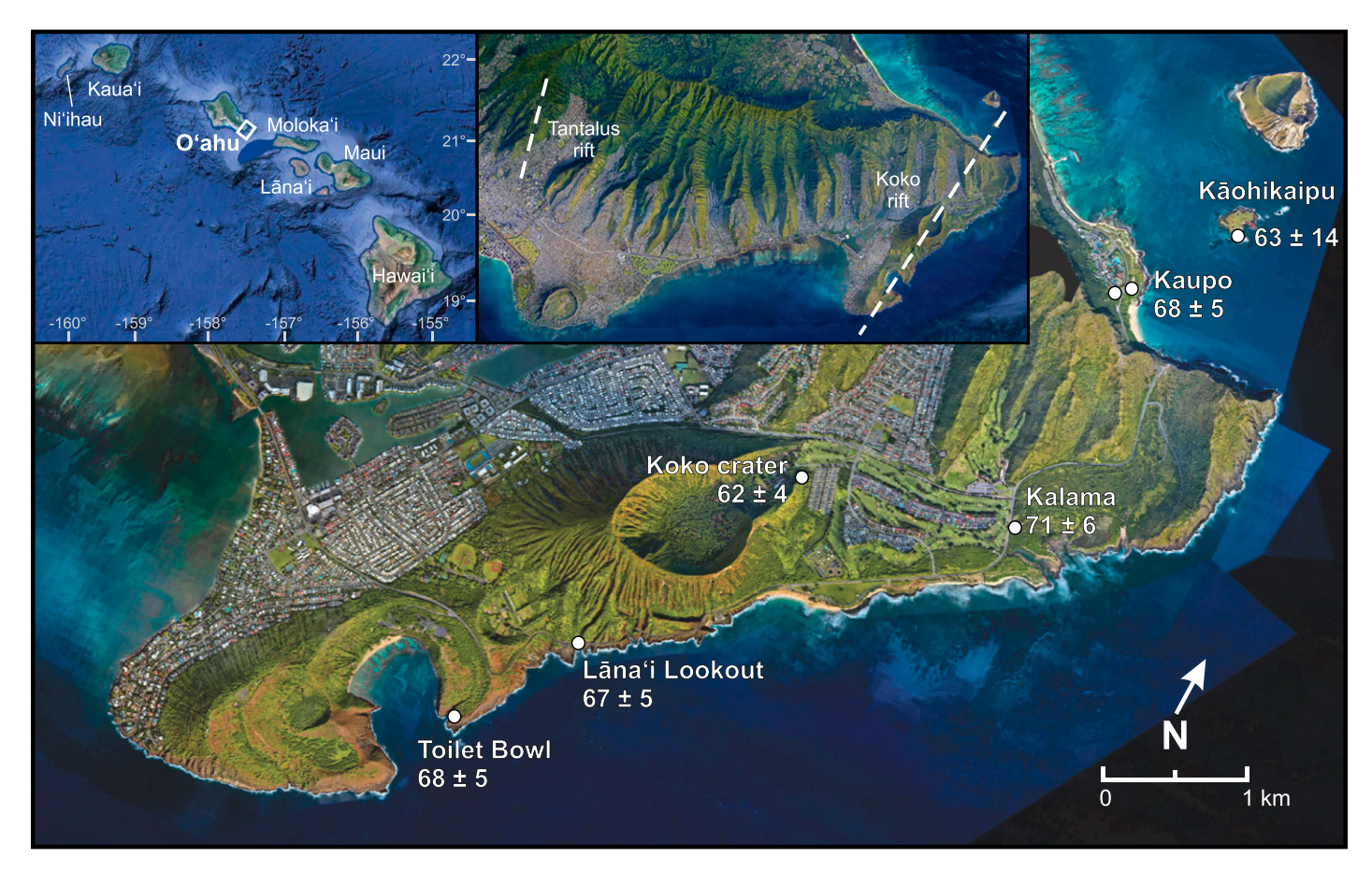


Figure 1. Locations for the <sup>40</sup>Ar/<sup>39</sup>Ar dated Koko Rift samples shown on a Google Earth image. Left inset shows the locations of the Hawaiian Islands mentioned throughout the text. White box in the inset encloses the Koko Rift on the southeastern side of Oʻahu. Right inset show the locations of the Koko and Tantalus rifts on Oʻahu. This figure was modified from Garcia et al. (2022). Google Earth images, including those in the insets, are courtesy of the U.S. Geological Survey, and the School of Ocean and Earth Science and Technology, University of Hawaiʾi at Manoa.

diffusion modeling presented here are new and were not presented in Garcia et al. (2022).

#### KOKO RIFT GEOLOGY AND SAMPLES

The ~18-km-long Koko Rift is the best developed rejuvenation stage rift system in Hawai'i. The subaerial portion of the Koko Rift has seven major vents and numerous subsidiary vents (Steams and Vaksvik, 1935). Several submarine cones lie along the same trend but are offset 0.5 km southwest of the subaerial Koko Rift (Clague et al., 2006). Volcanism along the currently subaerial section of the rift started in shallow water in the south blasting out chunks of coral reef and the underlying Koʻolau shield stage basalt until subaerial cones and a few short alkalic basalt lava flows were erupted (Wentworth, 1926). Eruptions on the northern end of the rift were subaerial and also produced alkalic basalt lavas.

The five larger Koko Rift subaerial flows we studied (Fig. 1) include three samples ana-

lyzed by Ozawa et al. (2005). These are Kalama (the largest flow along the Koko Rift), Kaupo (another large flow that extruded from a fissure in a cliff near Makapuu Point), and the socalled Toilet Bowl flow (a narrow, 600-m-long flow that extruded from a fissure between the inner and outer rims of the Hanauma Bay tuffcone complex, another major tourist attraction). Four other samples analyzed here are from Koko Crater; Lāna'i Lookout (another narrow, ~600-m-long flow that formed from a fissure on the southwestern flank of Koko Crater); Kāohikaipu Island, located ∼1 km to the north of the Kaupo flow at the northern end of the Koko Rift; and another sample from the Kaupo flow collected in 2018 (Fig. 1). All of these flows are larger than shown on maps, as most of the Koko Crater flow is buried by tephra, and the other flows are either partially underwater (Kaupo and Kalama) or were terminated by marine erosion (Lāna'i Lookout and Toilet Bowl).

Evidence for the relative age of Koko Rift eruptions is scant. For example, the path of the Kalama flow was apparently deflected by Koko Crater, but Koko tephra overlie the Kalama flow (Winchell, 1947). Furthermore, there are no soil horizons separating Koko Rift tephra or flows, although locally there are unconformities within the tephra sequence that indicate migration of vent locations and slumping (Wentworth, 1926). Previous studies have concluded that the volcanism along the Koko Rift was essentially coeval and may have occurred within weeks or possibly months based on similar modern eruptions (Wentworth, 1926; Winchell, 1947).

Whole-rock and mineral chemical data from Koko Rift basalts suggest that they were not in equilibrium with the mantle (Garcia et al., 2022). For example, the moderate forsterite contents of the olivines (80–85%) in the high MgO Koko basalts (10–11 wt.%) indicate that they underwent substantial crystal fractionation (Garcia et al., 2022). In addition, two of the Koko

flows that were dated (Toilet Bowl and Lāna'i Lookout) have only moderate MgO contents (5–6 wt%), which also indicates that they did not arise rapidly from the mantle.

#### **METHODS**

### 40Ar/39Ar Geochronology

Samples were taken from the dense interior of the lavas to avoid quenched outer rinds and/ or sections with abundant vesicles. Thin section inspection reveals no clays or calcite. Groundmass of the samples was isolated by crushing, sieving to 180-250 µm, magnetic sorting, and density separation using methylene iodide. The separates were then ultrasonically leached in 3 M HCl for 10 minutes, rinsed repeatedly with deionized water, and hand-picked under a binocular microscope to remove any altered material or phenocrysts. The hand-picked, purified separates were wrapped in Al foil, placed in 2.5 cm Al disks, and irradiated in the cadmium-lined incore tube at the Oregon State University reactor in Corvallis, Oregon, USA. The 1.1864 Ma Alder Creek sanidine (Jicha et al., 2016) was used as a neutron fluence monitor for all irradiations that spanned 1.5-6 h.

<sup>40</sup>Ar/<sup>39</sup>Ar analyses were conducted in the WiscAr Laboratory at the University of Wisconsin-Madison in Madison, Wisconsin, USA. Purified groundmass (20-30 mg) was incrementally heated with a 60 W CO<sub>2</sub> laser, and the gas was cleaned via exposure to two SAES GP50 getters in series (both at 50 W/400 °C) for 180 s each and to an ARS cryotrap (at -125 °C) for another 60 s. Isotopic analyses were done using a Nu Instruments Noblesse mass spectrometer. Sample analyses consisted of a continuous measurement for >1000 s to improve counting statistics, whereas blank and gas cocktail measurements were made with a peak hop routine (Jicha et al., 2016). Because it is critical to assess any subtle changes in instrument/background conditions during analyses of young mafic lavas, we measured a blank and a reference "in-house" gas cocktail before and after every sample analysis (Jicha et al., 2016). Most samples were analyzed more than once to assess reproducibility and improve precision. All of the <sup>40</sup>Ar/<sup>39</sup>Ar ages were calculated using the decay constants of Min et al. (2000) and are reported with  $2\sigma$  analytical uncertainties, which include the J uncertainty. All data were reduced and plotted using Pychron software (Ross, 2019). Only the plateau steps were used to calculate the isochrons. Heating steps that have suffered Ar loss, Ar recoil, or contain excess Ar should not fall along an isochron by definition, and thus it would be inaccurate to include them in the

isochron age calculation. For complete data, see Supplemental Table S1<sup>1</sup>.

#### **Olivine Diffusion Modeling**

Olivine cores and rims from 78 crystals from the Koko Rift eruptives (Koko Crater bomb and flow, Kaupo flow, and Kaohikaipu flow; Fig. 1) were analyzed for Si, Fe, Mg, Ni, and Ca using a JEOL JXA-8500F electron microprobe at the University of Hawai'i at Manoa to determine compositional populations. Garcia et al. (2022) reported olivine analyses (table 2 therein) for the Koko Crater bomb, Koko Crater flow, Kaupo flow, and Kāohikaipu Island. Here, we retrieved compositional profiles of 39 olivine phenocrysts (including the megacryst of olivine reported in table 2 of Garcia et al., 2022) from the same samples and conducted diffusion modeling work based on criteria aimed at reducing sectioning effects on apparent 2-D zoning in thin section (e.g., away from crystal corners and merging chemical zoning fronts; Shea et al., 2015). Profiles consisting of 30-80 closely spaced spot analyses of Fo (Mg/[Mg + Fe]) and Ni were also acquired with an accelerating voltage of 20 keV and a beam current of 200 nA (Table S2; see footnote 1). The counting times were 60 s on the peak and 30 s on the background on both sides of the peak. The beam size was 4–6 μm, depending on the size of the grain analyzed. Each profile consisted of at least 25 spot analyses.

#### **RESULTS**

Fourteen incremental heating experiments on lava from all six Koko Rift localities produced plateau ages ranging from  $62 \pm 4$  ka (Koko Crater) to  $71 \pm 6$  ka (Kalama) (Figs. 1 and 2 and Table 1). Because all of the isochrons have intercepts that are within uncertainty of the atmospheric value (Fig. 2), the plateau ages are preferred. Complete argon isotope data and reactor-induced corrections are provided in Table S1. The weighted mean of all the new plateau ages is  $66.5 \pm 2.1$  ka (MSWD = 1.05), which indicates that the Koko Rift eruptions are analytically indistinguishable in age, consistent with the interpretations of Winchell (1947) and Stearns and Vaksvik (1935). The new data are also indistinguishable from the K-Ar ages of Ozawa et al. (2005;  $60 \pm 90$ – $100 \pm 60$  ka) but significantly more precise. The new age,  $67 \pm 2$  ka, clearly establishes that the Koko Rift is the youngest site of rejuvenated volcanism in the Hawaiian Islands.

Zoning profiles were made on olivine in Koko basalts to assess their storage times in the magma prior to eruption. Most Koko olivine crystals are zoned normally from forsterite (Fo)<sub>81-85</sub> (mode at Fo<sub>84</sub> for olivine cores) to Fo<sub>79-83</sub> (mode at Fo<sub>82</sub> for olivine rims; Fig. S1A; see footnote 1). This zoning is overprinted by thin ( $<5 \mu m$ ), Fe-rich rims within lava flow samples (Kaupo and Kaohikaipu; Figs. 3C and 3D) as a result of post-eruptive, late-stage cooling during lava emplacement. Only one large olivine xenocryst (Fo<sub>88</sub>) was found in the Koko Crater bomb sample. All but two of the 39 olivines analyzed show normal zoning toward the rim. Most olivines with clear plateaus both at the core and at the rim exhibit a sigmoidal shape (Fig. S1C), which indicates that crystal rims formed in equilibrium with the surrounding melt. Less common and more complex, some olivines show both normal and reverse zoning and record a multistage diffusion history that suggests chemical fluctuations of the melt.

Diffusion modeling of Fo and Ni concentration gradients in the olivine crystals yielded a broad range of timescales with an average of  $\sim$ 200 days (Figs. 3A and 3B). Timescales extracted from Fo profiles span from 32 days to 3140 days; those derived from Ni range between 26 days and 3936 days. Generally, the diffusion timescales for Fo and Ni concur ( $R^2 = 0.85$ ; Fig. 3B). Thus, the oliving zoning profiles suggest that most Koko basaltic magmas were likely stored in the crust for months to years (up to 10.8 yr) prior to their eruption. Precisely constraining where the Koko Rift magmas were stored within the relatively thin Hawaiian crust ( $\sim$ 15 km; Watts and Ten Brink, 1989) is difficult, because calibrated mineral barometers, such as the clinopyroxene-melt barometer, are inaccurate when applied to mafic magmas. Moreover, the cpx-melt barometer assumes the clinopyroxene was in equilibrium (Putirka et al., 2003), and the complex zoning of the Koko Rift clinopyroxenes clearly shows they were out of equilibrium (Garcia et al., 2022). For these reasons, we use the term "in the crust" herein to reflect Koko magma storage at depths of < 15 km.

No mantle xenoliths have been found in Koko basalts, which supports the suggestion that Koko magmas were stored in the crust for months to years and did not rapidly rise from the mantle in a few hours as has been estimated for other xenolith-bearing Honolulu eruptions such as Salt Lake Crater (Peslier et al., 2015).

¹Supplemental Material. Table S1: Complete ⁴⁰Ar/³⁰Ar data. Table S2: Fo (=Mg/[Mg + Fe]) and Ni EPMA data for olivine profiles from the Koko Rift (Koko Crater bomb and flow, Kaupo lava flow and Kāohikaipu Island) from core to rim. Please visit https://doi.org/10.1130/GSAB.21445722 to access the supplemental material, and contact editing@geosociety.org with any questions.

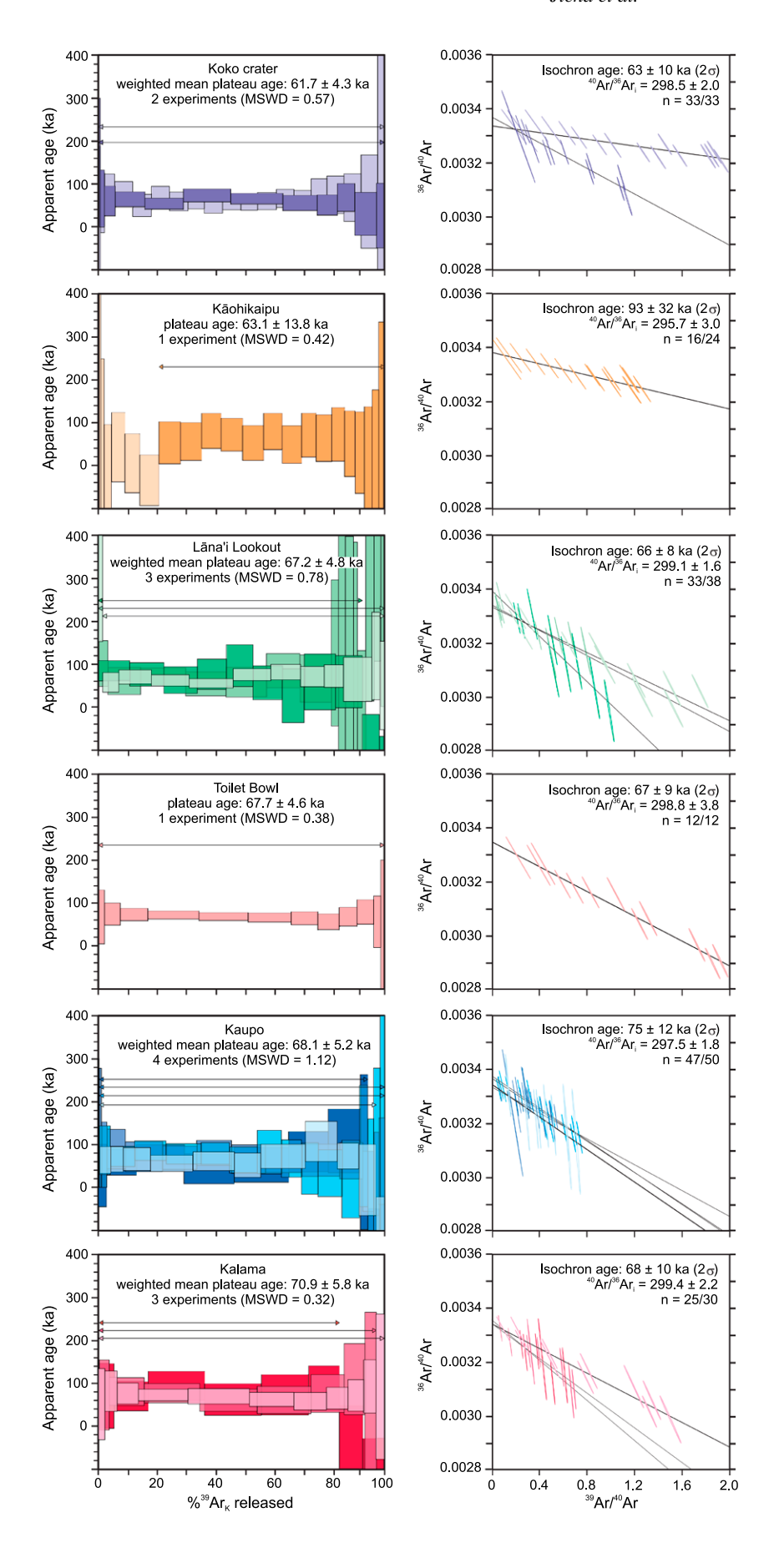


Figure 2. 40Ar/39Ar age spectrum and isochron diagrams are shown. All six Koko Rift lavas produced plateau ages ranging from  $62 \pm 4$  ka (Koko Crater) to  $71 \pm 6$  ka (Kalama). A weighted mean of all 14 new plateau ages is  $66.5 \pm 2.1$  ka (MSWD = 1.05), which indicates that the Koko Rift eruptions are analytically indistinguishable. All individual heating steps and plateau ages are shown with 2σ uncertainties. Plateau steps are used to calculate the isochrons. Individual isochrons are shown where multiple experiments were conducted for a sample. Different isochron slopes reflect different irradiation durations. MSWD-mean square of weighted deviates.

# MECHANISMS FOR REJUVENATED VOLCANISM AND THE TRIGGER FOR KOKO RIFT ERUPTIONS

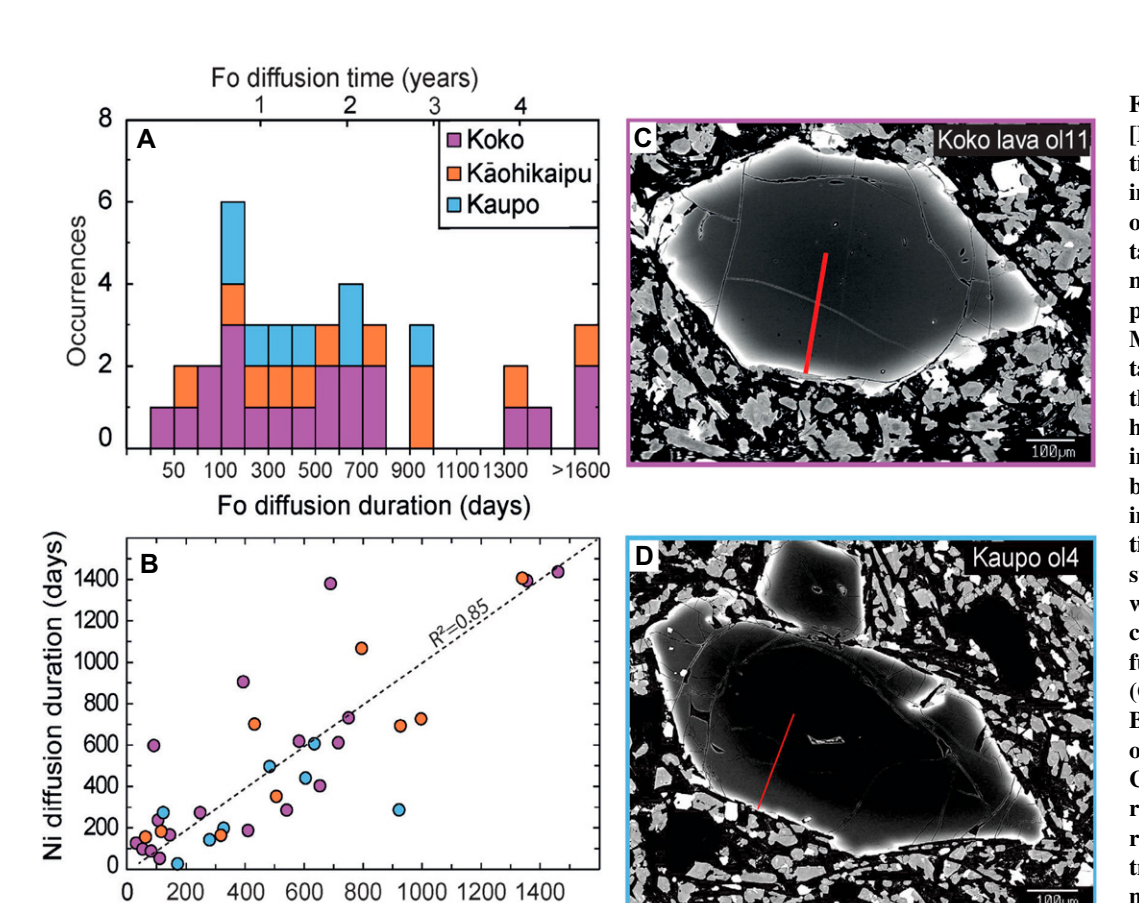
The cause of Hawaiian rejuvenated volcanism remains controversial because all of the proposed mechanisms fail to explain either their timing and/or volume (Garcia et al., 2010). One of these mechanisms, flexural uplift, was proposed to explain Koko Rift volcanism (Ozawa et al., 2005). Uplift of the Ko'olau shield volcano was associated with rapid loading of the lithosphere by the new, growing shield volcano (Mauna Loa; Bianco et al., 2005). The timing of this mechanism is potentially suitable for the early stages of Honolulu volcanism, when uplift and melting would have been greatest. However, flexural uplift of O'ahu probably ended at ca. 100 ka assuming a plate velocity of  $\sim$ 10 cm/ yr and an elastic plate thickness of  $\sim$ 25 km (Bianco et al., 2005). Thus, it is not a likely explanation for the timing of Koko volcanism at ca. 67 ka.

The secondary plume melting zone model (e.g., Ribe and Christensen, 1999) does explain the timing of Honolulu volcanism and its most recent products along the Koko Rift (Fig. 4). Melt generation in this geodynamic model occurs as the plume ascends and spreads laterally. Secondary melting is predicted to occur  $\sim$ 300–520 km downstream of the plume's vertical stem (Fig. 4). Koko Rift is currently ~350 km away from the inferred Hawaiian plume stem and is consistent with this model. Furthermore, this model predicts that rejuvenated volcanism may continue in Honolulu for another million years, comparable with the duration of rejuvenated volcanism on the northern Hawaiian Islands of Kaua'i, Ka'ula, and Ni'ihau (ca. 1.5-2.5 Ma; Garcia et al., 2016). Thus, we suggest that the secondary plume melting model is likely responsible for Koko Rift magma generation. However,

TABLE 1. SUMMARY OF 40 Ar/39 Ar DATA

IABLE I. SUMINART OF "AII" ALDAIA													
Location /	Latitude	Longitude	K/Ca	$^{40}$ Ar/ $^{36}$ Ar $_{ m i}\pm2\sigma$		Isochron age		MSWD	N	<sup>39</sup> Ar%	MSWD		au age
sample no.	(°N)	(°W)	total			(ka) $\pm$ 2 $\sigma$						(ka)	± <b>2</b> σ
Koko Crater													
Koko3	21.2927	157.6762	0.142	299.7	$\pm 2.5$	55	$\pm 15$	0.40	20/20	100.0	0.41	62.0	$\pm 6.2$
			0.236	296.4	$\pm 3.4$	69	$\pm 13$	0.82	13/13	100.0	0.88	61.4	$\pm 6.1$
					weighted mean:	63	$\pm 10$		33/33		0.57	61.7	$\pm 4.3$
Kaohikapu													
Kaohi-2	21.31957	157.6557	0.053	295.7	±3.0	93	±32	0.20	16/24	78.8	0.42	63.1	±13.8
<u>Lāna'i Lookout</u> Lāna'i Lookout	21.2769	157.6850	0.153	295.1	±5.4	86	±22	0.57	9/11	92.3	0.70	73.7	±12.2
Lana i Lookout	21.2703	137.0030	0.155	299.4	±1.9	64	±15	0.57	13/15	96.4	0.76	68.5	±12.2 ±12.0
			0.030	299.9	±3.7	62	±13 +10	1.24	11/12	98.5	1.15	65.3	±12.0 ±6.1
			0.124	233.3	$\pm$ 3.7 weighted mean:	66	±10 ±8	1.24	33/38	30.5	0.78	67.2	±4.8
					weignieu mean.	00	<b>±0</b>		33/30		0.76	07.2	±4.0
Toilet Bowl													
HV-02-08	21.2701	157.6903	0.176	298.8	±3.8	67	$\pm 9$	0.43	12/12	100.0	0.38	67.7	$\pm 4.6$
Kaupo													
Kaupo	21.3125	157.6618	0.256	299.2	$\pm 8.0$	62	$\pm 64$	0.32	10/11	96.5	0.81	64.5	$\pm 8.8$
·			0.233	300.1	$\pm 3.7$	50	±26	0.71	8/10	90.9	0.70	61.5	$\pm 15.0$
			0.111	297.4	$\pm 1.8$	82	±15	0.54	15/15	100.0	0.61	74.9	$\pm 9.9$
MP-18-06	21.31327	157.6609	0.193	296.4	±5.7	86	±39	0.43	14/14	100.0	0.44	68.8	±11.5
					weighted mean:	75	±12		47/50		1.11	68.1	$\pm 5.2$
<u>Kalama</u> Kalama	21.2954	157.6620	0.046	299.4	±3.9	69	±22	0.41	8/10	97.2	0.37	72.8	±12.6
Naiama	21.2354	137.0020	0.046	298.1	±3.9 ±8.7	79	±46	0.52	6/9	84.0	0.37	76.2	±17.1
			0.216	299.5	±8.7 ±3.0	66	±46 ±12	0.36	11/11	100.0	0.41	69.4	
			0.237	299.5		68		0.30	25/30	100.0	0.36	70.9	±7.2
					weighted mean:	80	$\pm 10$		25/30		0.32	70.9	$\pm 5.8$

Note: Ages were calculated relative to 1.1864 Ma Alder Creek sanidine standard (Jicha et al., 2016) using the decay constants of Min et al. (2000). Atmospheric  $^{40}$ Ar/ $^{36}$ Ar = 298.56  $\pm$  0.62 (Lee et al., 2006);  $^{40}$ Ar/ $^{36}$ Ar<sub>i</sub> = trapped initial  $^{40}$ Ar/ $^{36}$ Ar. N—number of plateau steps/number of total incremental heating steps; points used to calculate isochron = number of plateau steps. Sample HV-02-08 was mislabeled as Hanauma by Ozawa et al. (2005) but is from the so-called Toilet Bowl flow. MSWD—mean square of weighted deviates.



Fo diffusion duration (days)

Figure 3. Forsterite (Fo = Mg/[Mg + Fe]) and Ni diffusion timescales for Koko Rift olivine are plotted. (A) Histogram of the Fo diffusion time obtained using finite difference modeling of 1-D compositional profiles (see **Supplemental** Material text for modeling details; see text footnote 1). Note that the first four bins of the histogram represent 25 day increments, but subsequent bins are divided into 100 day increments. (B) Diffusion durations of Ni versus Fo. Note the sub-linear trend  $(R^2 = 0.85)$ , which indicates that the chemical gradients result from diffusion rather than growth (Costa et al., 2020). (C and D) **Back-scattered electron images** of olivine crystals from Koko Crater and Kaupo lava flows, respectively. The red lines represent compositional profile transects obtained for diffusion modeling.

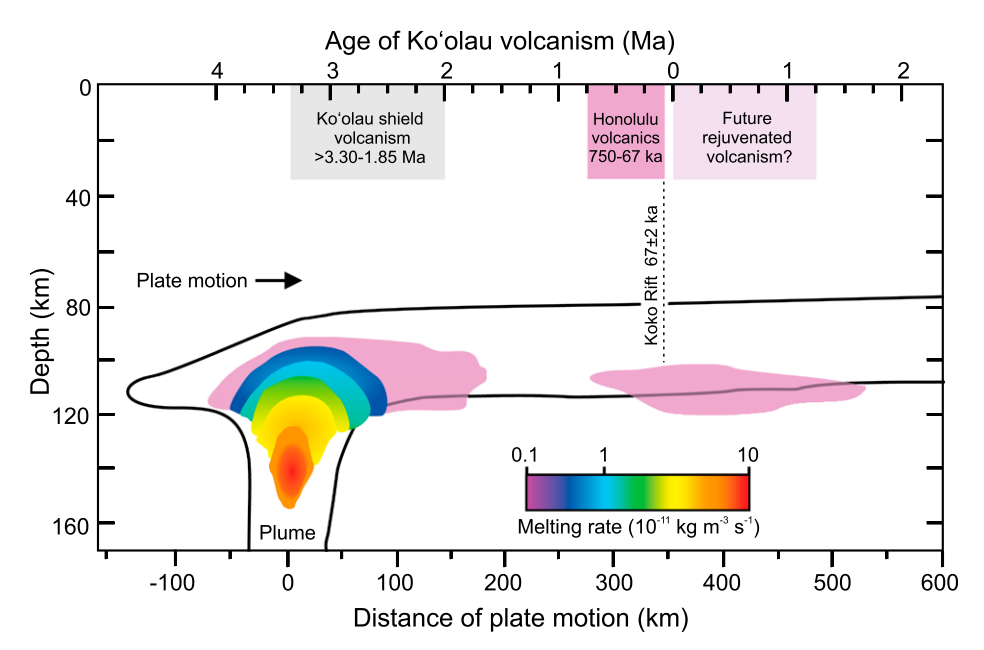


Figure 4. Conceptual model of Honolulu rejuvenated volcanism that is modified from Ribe and Christensen (1999). Melting rate is a function of distance from the plume. Available ages of Koʻolau and Honolulu volcanism are shown (top). Black lines are streamlines for the plume flow, which is inferred to rise laterally away from the plume stem by the northwestward motion of the Pacific lithosphere, and which causes secondary melting.

an additional mechanism may have played a role in triggering the Koko Rift eruptions from within the crust.

Quaternary changes in sea level have been proposed to have a strong influence on the frequency and magnitude of eruptions of volcanoes in the Mediterranean Sea (McGuire et al., 1997). More recently, oscillations in sea level were recently recognized as a potential key mechanism for modulating volcanism by causing crustal stress from loading and unloading in oceanic regions (Crowley et al., 2015; Satow et al., 2021). A striking relationship between sea-level changes and the timing of eruptions was found at Santorini volcano, a Greek island in the Mediterranean Sea. Virtually all (208 of 211) eruptions of Santorini over the past 360 ka were attributed to a reduction in tensile stresses during low sea levels (Satow et al., 2021). Numerical modeling suggests that when the sea level falls by 40 m below the present-day level, dike injections are triggered (Satow et al., 2021). If sea level continues to fall to -70 mto  $-80 \,\mathrm{m}$ , the induced tensile stresses reach the surface of the volcano, and dike-fed eruptions occur, which suggests a strong absolute sea-level control on the timing of the Santorini eruptions (Satow et al., 2021). Geophysical and petrologic data suggest that the Santorini magma chamber is located at a depth of ~4 km beneath its caldera (Satow et al., 2021, and references therein).

One of the remarkable discoveries of this work is that at least some rejuvenation-stage magmas did not rise rapidly from the deep mantle. The moderate forsterite contents (80-84%) and modeling of the zoning profiles in Koko Rift olivines indicate that they were stored in the Hawaiian crust for many months to several years prior to eruption. In the Koko Rift area, the crust is <15 km (Watts and Ten Brink, 1989). It is difficult to precisely constrain where the Koko magmas were stored within the 15 km of crust for the reasons stated above and due to the lack of geophysical data along the rift. Using available geophysical data (Lindwall, 1988), the Koko magma may have been stored where there was a crustal density contrast at  $\sim$ 4 km or at  $\sim$ 10 km (i.e., near the top of the oceanic crust). Therefore, it is reasonable to assume that the Koko magma chambers may also have been located at < 10 km, similar to the depth of the Santorini magma chamber. Shallow (<10 km) Koko Rift magma chambers would also be consistent with the model of Satow et al. (2021), which requires the chamber to be located within the upper 9 km of crust where rock tensile strength is almost constant and tensile stresses induced by sea-level falls can become more pronounced. Could sea-level variation have triggered the Koko Rift eruptions?

The Koko Rift volcanism at ca. 67 ka occurred during or just after the >100 m drop in global sea level to -100 m during the onset of MIS4 (Grant et al., 2014; Spratt and Lisiecki, 2016;

Fig. 5). This is well below the -70 m to -80 msea-level threshold thought to be needed to induce dike-fed eruptions at Santorini. Interestingly, the Skaros lavas were emplaced at Santorini at ca. 67 ka (Druitt et al., 1999), and several closely spaced alkaline eruptions occurred at ca. 53-72 ka on Ascension Island (Jicha et al., 2013; Preece et al., 2021), which suggests that sea-level fall may have promoted eruptions from volcanic islands in the Atlantic, Mediterranean, and Pacific at this time. It is important to note that given the uncertainties the ages of dated deposits, it has been difficult to assess, thus far, how much time may have elapsed between a sealevel change below the proposed threshold and the eruption.

To further interrogate the timing of eruptions and the relative sea level, we evaluated the available geochronologic data from numerous other oceanic island volcanoes (Fogo, Samoa, and Tristan da Cunha). There are numerous dated eruptions on Fogo, Tristan da Cunha, and Ascension over the last 400 ka. We used kernel density estimates (the same approach used by Satow et al., 2021) to identify peaks in volcanic activity on these islands because this approach considers the uncertainties associated with the dated eruptions. Ages of individual eruptions are also shown in Figure 5 for Kaua'i, Moloka'i, Samoa, and the Tantalus Rift. While there were undoubtedly many more eruptions on other oceanic islands during this time period, the ages of those eruptions are unknown or not precisely dated and therefore are not used in this compilation.

Overall, eruptions or peaks in volcanic activity primarily occurred during sea-level lows during the last 400 ka (Fig. 5). Sea-level change may have also triggered rejuvenated volcanism on other Hawaiian islands (Kaua'i and Moloka'i) throughout the mid–late Pleistocene (Fig. 5). Precise dating of the ca. 750–100 ka Honolulu eruptions is needed to evaluate this correlation more fully.

# HAZARD IMPLICATIONS AND CONCLUSIONS

Rejuvenated eruptions pose a significant hazard for populated areas given the likelihood of limited precursor activity before an eruption (Peslier et al., 2015). This is especially important because there may be many tens of thousands of years between eruptions. The Tantalus and Koko Rift eruptions were preceded by the Honolulu eruptions at ca. 200–300 ka (Ozawa et al., 2005). Given the episodic nature of the rejuvenated volcanism on Oʻahu and the potential for it to continue well into the future (Fig. 4), it is plausible to assume that future eruptions could occur in the Honolulu area.

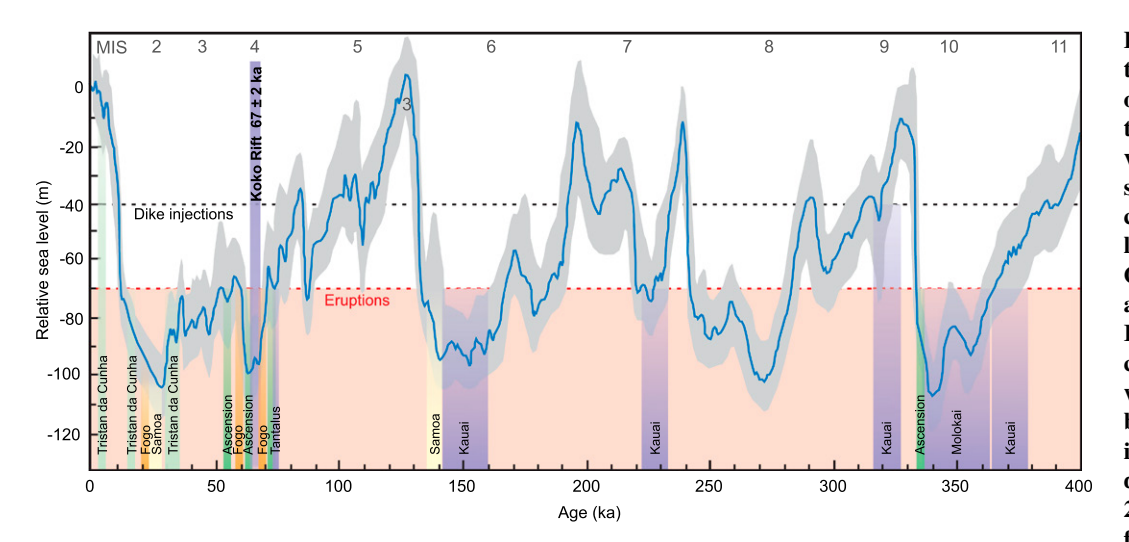


Figure 5. Sea-level changes over the last 400 ka and the timing of Koko Rift eruptions and those from other ocean island volcanoes are plotted. Relative sea level (blue line) and 95% confidence interval (gray envelope) versus age; modified from Grant et al. (2014). Numbers along the top refer to Marine Isotope Stages (MIS). Numerical modeling indicates that when the sea level falls 40 m below the present-day level, the induced tensile stresses trigger dike injections (Satow et al., 2021). If sea level continues to fall to -70 m or -80 m, the in-

duced tensile stress is inferred to allow dikes to reach the surface and erupt. Koko Rift volcanism occurred at  $66.5 \pm 2.1$  ka, when sea level dropped to -100 m during the MIS 4 glacial. This may have triggered Koko Rift rejuvenated volcanism. Other recently dated Hawaiian rejuvenated volcanism (purple) as well as eruptions from Fogo (orange), Samoa (yellow), Tristan da Cunha (light green), and Ascension Island (dark green) are shown, which primarily occur during sea-level lows with the exception of the ca. 323 ka lavas on Kaua'i and ca. 4 ka post-shield scoria cones on Tristan da Cunha (Hicks et al., 2012). For Fogo, Tristan da Cunha, and Ascension, the ages represent peaks in kernel density functions, where ages of individual eruptions are shown for Kaua'i, Moloka'i, Samoa, and the Tantalus Rift. Historic eruptions are not considered as the focus is on the relationship between ocean island volcanism and late Pleistocene sea-level changes. Data sources: (Jicha et al., 2013; Preece et al., 2021; Garcia et al., 2010; Clague et al., 2016; Cornu et al., 2021; Gale et al., 2021; Reinhard et al., 2019; Hicks et al., 2012; Hearty et al., 2005; and Clague et al., 1982).

The new <sup>40</sup>Ar/<sup>39</sup>Ar chronology and diffusion modeling in olivine in Koko Rift basalts has allowed us to refine the timing and recurrence of Honolulu rejuvenated volcanism, and to re-visit and propose a potential triggering mechanism. Future investigations of rejuvenated volcanism in Hawai'i and globally should also consider the long-term influence of the Earth's climate system on magmatic processes to better infer past and future eruptive behavior.

#### ACKNOWLEDGMENTS

Kierstin Swanson initiated our interest in the Koko Rift and collected several of the samples used in this study. This study builds on the work of Jack Naughton and Ian McDougall, who were pioneers in determining ages for Hawai'i's notoriously difficult-to-date rocks. This study was partially supported by National Science Foundation grants OCE-1834723 and OCE-1834758. We thank Mark Stelten and John Smellie for very helpful reviews. This is School of Ocean and Earth Science and Technology, University of Hawai'i at Manoa, contribution 11587.

#### REFERENCES CITED

Bianco, T.A., Ito, G., Becker, J.M., and Garcia, M.O., 2005, Secondary Hawaiian volcanism formed by flexural arch decompression: Geochemistry, Geophysics, Geosystems, v. 6, https://doi.org/10.1029/2005GC000945.

Clague, D.A., and Frey, F.A., 1982, Petrology and trace element geochemistry of the Honolulu Volcanics, Oahu: Implications for the oceanic mantle below Hawaii: Journal of Petrology, v. 23, p. 447–504, https://doi.org/10.1093/petrology/23.3.447.

Clague, D.A., Dao-Gong, C., Murnane, R., Beeson, M.H., Lanphere, M.A., Dalrymple, G.B., Friesen, W., and Holcomb, R.T., 1982, Age and petrology of the Kalaupapa basalt, Molokai, Hawaii: Pacific Science, v. 36, p. 411–420.

Clague, D.A., Paduan, J.B., McIntosh, W.C., Cousens, B.L., Davis, A.S., and Reynolds, J.R., 2006, A submarine perspective of the Honolulu Volcanics, Oahu: Journal of Volcanology and Geothermal Research, v. 151, p. 279– 307, https://doi.org/10.1016/j.jvolgeores.2005.07.036.

Clague, D.A., Frey, F.A., Garcia, M.O., Huang, S., McWilliams, M., and Beeson, M.H., 2016, Compositional heterogeneity of the Sugarloaf mellite nephelinite flow, Honolulu Volcanics, Hawai'i: Geochimica et Cosmochimica Acta, v. 185, p. 251–277, https://doi.org/10.1016/j.gca.2016.01.034

Cornu, M.N., Paris, R., Doucelance, R., Bachèlery, P., Bosq, C., Auclair, D., Benbakkar, M., Gannoun, A.M., and Guillou, H., 2021, Exploring the links between volcano flank collapse and the magmatic evolution of an ocean island volcano: Fogo, Cape Verde: Scientific Reports, v. 11, p. 1–12, https://doi.org/10.1038/s41598-021-96897-1.

Costa, F., Shea, T., and Ubide, T., 2020, Diffusion chronometry and the timescales of magmatic processes: Nature Reviews. Earth & Environment, v. 1, p. 201–214, https://doi.org/10.1038/s43017-020-0038-x.

Crowley, J.W., Katz, R.F., Huybers, P., Langmuir, C.H., and Park, S.H., 2015, Glacial cycles drive variations in the production of oceanic crust: Science, v. 347, p. 1237– 1240, https://doi.org/10.1126/science.1261508.

Dana, J.D., 1849, Geology, in Wilkes, C., United States Exploring Expedition 10, Philadelphia, C. Sherman, with atlas: New York, Putnam, https://doi.org/10.5962/bhl.title.68069.

Druitt, T.H., Edwards, L., Mellors, R.M., Pyle, D.M., Sparks, R.S.J., Lanphere, M., Davies, M., and Barreirio, B., 1999, Santorini Volcano: Geological Society Memoir 19, 165 p.

Dutton, C.E., 1884: Hawaiian volcanoes: U.S. Geological Survey Annual Report 4, 145 p.

Gale, S.J., Miggins, D.P., and Fepuleai, A., 2021, 40Ar/39Ar dating of Quaternary volcanic rocks in Samoa: New Zealand Journal of Geology and Geophysics, v. 65, p. 381–388, https://doi.org/10.1080/00288306.2021.1929348.

Garcia, M.O., Swinnard, L., Weis, D., Greene, A.R., Tagami, T., Sano, H., and Gandy, C.E., 2010, Petrology, geochemistry and geochronology of Kaua'i lavas over 4–5 Myr: Implications for the origin of rejuvenated volcanism and the evolution of the Hawaiian plume: Journal of Petrology, v. 51, p. 1507–1540, https://doi.org/10.1093/petrology/egq027.

Garcia, M.O., Weis, D., Jicha, B.R., Ito, G., and Hanano, D., 2016, Petrology and geochronology of lavas from Ka'ula volcano: Implications for rejuvenated volcanism of the Hawaiian mantle plume: Geochimica et Cosmochimica Acta, v. 185, p. 278–301, https://doi.org/10 .1016/j.gca.2016.03.025.

Garcia, M.O., Swanson, K., Lormand, C., and Norman, M.D., 2022, Petrology of Koko Rift basalts: Hawai'i's most recent and atypical rejuvenation stage eruptive sequence: Journal of Volcanology and Geothermal Research, v. 424, https://doi.org/10.1016/j.jvolgeores .2022.107504.

Geldmacher, J., and Hoernle, K., 2000, The 72 Ma geochemical evolution of the Madeira hotspot (eastern North Atlantic): Recycling of Paleozoic (≤500 Ma) oceanic lithosphere: Earth and Planetary Science Letters, v. 183, p. 73–92, https://doi.org/10.1016 /S0012-821X(00)00266-1.

Gramlich, J.W., Lewis, V.A., and Naughton, J.J., 1971, Potassium-argon dating of Holocene basalts of the Honolulu Volcanic Series: Geological Society of America Bulletin, v. 82, p. 1399–1404, https://doi.org/10.1130 //0016-7606(1971)82[1399:PDOHBO]2.0.CO;2.

Grant, K.M., Rohling, E.J., Bronk Ramsey, C., Cheng, H., Edwards, R.L., Florindo, F., Heslop, D., Marra, F., Roberts, A.P., Tamisiea, M.E., and Williams, F., 2014. Sea-level variability over five glacial cycles: Nature Communications, v. 5, 5076, https://doi.org/10.1038/ncomms6076.

Hearty, P.J., Karner, D.B., Renne, P.R., Olson, S.L., and Fletcher, S., 2005, 40Ar/39Ar age of a young rejuvenation basalt flow: Implications for the duration of volcanism and the timing of carbonate platform development during the Quaternary on Kaua'i, Hawaiian Islands: New Zealand Journal of Geology and Geophysics, v. 48, p. 199–211, https://doi.org/10.1080/00288306 .2005.9515110.

- Heizler, M.T., Perry, F.V., Crowe, B.M., Peters, L., and Appelt, R., 1999, The age of Lathrop Wells volcanic center: An <sup>40</sup>Ar/<sup>39</sup>Ar dating investigation: Journal of Geophysical Research, v. 104, p. 767–804, https://doi .org/10.1029/1998JB900002.
- Hicks, A., Barclay, J., Mark, D.F., and Loughlin, S., 2012, Tristan da Cunha: Constraining eruptive behavior using the <sup>40</sup>Ar/<sup>39</sup>Ar dating technique: Geology, v. 40, p. 723– 726, https://doi.org/10.1130/G33059.1.
- Jicha, B.R., Singer, B.S., and Valentine, M.J., 2013, 40Ar/39Ar geochronology of subaerial Ascension Island and a re-evaluation of the temporal progression of basaltic to rhyolitic volcanism: Journal of Petrology, v. 54, p. 2581–2596, https://doi.org/10.1093/petrology /egt058.
- Jicha, B.R., Singer, B.S., and Sobol, P., 2016, Re-evaluation of the ages of <sup>40</sup>Arf<sup>39</sup>Ar sanidine standards and supereruptions in the western U.S. using a Noblesse multi-collector mass spectrometer: Chemical Geology, v. 431, p. 54–66, https://doi.org/10.1016/j.chemgeo.2016.03.024.
- Konter, J., and Jackson, M.G., 2012, Large volumes of rejuvenated volcanism in Samoa: Evidence supporting a tectonic influence on late-stage volcanism: Geochemistry, Geophysics, Geosystems, v. 13, https://doi.org/10 .1029/2011GC003974.
- Lanphere, M.A., and Dalrymple, G.B., 1980, Age and strontium isotopic composition of the Honolulu volcanic series, Oahu, Hawaii: American Journal of Science, v. 280A, p. 736–751.
- Lee, J.-Y., Marti, K., Severinghaus, J.P., Kawamura, K., Yoo, H.-S., Lee, J.B., and Kim, J.S., 2006, A redetermination of the isotopic abundance of atmospheric Ar: Geochimica et Cosmochimica Acta, v. 70, p. 4507–4512, https:// doi.org/10.1016/j.gca.2006.06.1563.
- Lindwall, D.A., 1988, A two-dimensional seismic investigation of crustal structure under the Hawaiian Islands near Oahu and Kauai: Journal of Geophysical Research: Solid Earth, v. 93, p. 12,107–12,122, https://doi.org/10.1029/JB093iB10p12107.
- McGuire, W.J., Howarth, R.J., Firth, C.R., Solow, A.R., Pullen, A.D., Saunders, S.J., Stewart, I.S., and Vita-Finzi, C., 1997, Correlation between rate of sea-level change and frequency of explosive volcanism in the Mediterranean: Nature, v. 389, p. 473–476, https://doi.org/10.1038/38998.
- Min, K., Mundil, R., Renne, P.R., and Ludwig, K.R., 2000, A test for systematic errors in <sup>40</sup>Ar/<sup>39</sup>Ar geochronology through comparison with U/Pb analysis of a 1.1-Ga rhy-

- olite: Geochimica et Cosmochimica Acta, v. 64, p. 73–98, https://doi.org/10.1016/S0016-7037(99)00204-5.
- Ozawa, A., Ragami, T., and Garcia, M.O., 2005, Unspiked K-Ar dating of the Honolulu rejuvenated and Koolau shield volcanism on Oahu, Hawaii: Earth and Planetary Science Letters, v. 232, p. 1–11, https://doi.org/10.1016/j.epsl.2005.01.021.
- Paul, D., White, W.M., and Blichert-Toft, J., 2005, Geochemistry of Mauritius and the origin of rejuvenescent volcanism on oceanic island volcanoes: Geochemistry, Geophysics, Geosystems, v. 6, https://doi.org/10.1029/ /2004GC000883.
- Peslier, A.H., Bizimis, M., and Matney, M., 2015, Water disequilibrium in olivines from Hawaiian peridotites: Recent metasomatism, H diffusion and magma ascent rates: Geochimica et Cosmochimica Acta, v. 154, p. 98–117, https://doi.org/10.1016/j.gca.2015 .01.030.
- Preece, K., Mark, D.F., Barclay, J., Cohen, B.E., Chamberlain, K.J., Jowitt, C., Vye-Brown, C., Brown, R.J., and Hamilton, S., 2018, Bridging the gap: <sup>40</sup>Arf<sup>39</sup>Ar dating of volcanic eruptions from the 'Age of Discovery': Geology, v. 46, p. 1035–1038, https://doi.org/10.1130/645415.1.
- Preece, K., Barclay, J., Brown, R.J., Chamberlain, K.J., and Mark, D.F., 2021, Explosive felsic eruptions on ocean islands: A case study from Ascension Island (South Atlantic): Journal of Volcanology and Geothermal Research, v. 416, https://doi.org/10.1016/j.jvolgeores .2021.107284.
- Putirka, K.D., Mikaelian, H., Ryerson, F., and Shaw, H., 2003, New clinopyroxene-liquid thermobarometers for mafic, evolved, and volatile-bearing lava compositions, with applications to lavas from Tibet and the Snake River Plain, Idaho: The American Mineralogist, v. 88, p. 1542–1554, https://doi.org/10.2138 /am-2003-1017.
- Reinhard, A.A., Jackson, M.G., Blusztajn, J., Koppers, A.A., Simms, A.R., and Konter, J.G., 2019, "Petit spot" rejuvenated volcanism superimposed on plume-derived Samoan shield volcanoes: Evidence from a 645-m drill core from Tutuila Island, American Samoa: Geochemistry, Geophysics, Geosystems, v. 20, p. 1485–1507, https://doi.org/10.1029/2018GC007985.
- Ribe, N., and Christensen, U., 1999, The dynamical origin of Hawaiian volcanism: Earth and Planetary Science Letters, v. 171, p. 517–531, https://doi.org/10.1016 /S0012-821X(99)00179-X.

- Ross, J., 2019, NMGRL/pychron v18.2: https://doi.org/10 .5281/zenodo.3237834.
- Satow, C., Gudmundsson, A., Gertisser, R., Ramsey, C.B., Bazargan, M., Pyle, D.M., Wulf, S., Miles, A.J., and Hardiman, M., 2021, Eruptive activity of the Santorini volcano controlled by sea-level rise and fall: Nature Geoscience, v. 14, p. 586–592, https://doi.org/10.1038 /s41561-021-00783-4.
- Shea, T., Lynn, K.J., and Garcia, M.O., 2015, Cracking the olivine zoning code: Distinguishing between crystal growth and diffusion: Geology, v. 43, p. 935–938, https://doi.org/10.1130/G37082.1.
- Spratt, R.M., and Lisiecki, L.E., 2016, A Late Pleistocene sea level stack: Climate of the Past, v. 12, p. 1079–1092, https://doi.org/10.5194/cp-12-1079-2016.
- Stearns, H.T., and Vaksvik, K.N., 1935, Geology and groundwater resources of the island of Oahu: Hawaii: Hawaii Division of Hydrography Bulletin, v. 1, 479 p.
- Szabo, B.J., Ludwig, K.R., Muhs, D.R., and Simmons, K.R., 1994, Thorium-230 ages of corals and duration of the last interglacial sea-level high stand on Oahu, Hawaii: Science, v. 266, p. 93–96, https://doi.org/10.1126/ science.266.5182.93.
- Watts, A.B., and Ten Brink, U.S., 1989, Crustal structure, flexure, and subsidence history of the Hawaiian Islands: Journal of Geophysical Research: Solid Earth, v. 94, no. B8, p. 10,473–10,500, https://doi.org/10.1029
- Weis, D., Frey, F.A., Giret, A., and Cantagrel, J.M., 1998, Geochemical characteristics of youngest volcano (Mount Ross) in the Kerguelen Archipelago; inferences for magma flux, lithosphere assimilation and composition of the Kerguelen Plume: Journal of Petrology, v. 39, p. 973–994, https://doi.org/10.1093/petroj/39.5.973.
- Wentworth, C.K., 1926, Pyroclastic geology of Oahu: B.P. Bishop Museum Bulletin, v. 30, 121 p.
- Winchell, H., 1947, Honolulu series, Oahu, Hawaii: Geological Society of America Bulletin, v. 58, p. 1–48, https://doi.org/10.1130/0016-7606(1947)58[1:HSOH]2 0.CO:2.

SCIENCE EDITOR: MIHAI DUCEA ASSOCIATE EDITOR: MICHAEL ORT

Manuscript Received 1 June 2022 Revised Manuscript Received 11 September 2022 Manuscript Accepted 26 October 2022

Printed in the US